TESTING OF SHEATHED COLD-FORMED STEEL STUD SHEAR WALLS FOR SEISMIC PERFORMANCE EVALUATION

R. Landolfo[1], G. Della Corte[2], L. Fiorino[3]

SUMMARY

The paper presents and discusses the results of an experimental investigation on the seismic response of sheathed cold-formed steel stud shear wall systems. Physical tests have been carried out on two, nominally identical, structural sub-assemblage, each of them composed by two sheathed stud walls. One prototype has been tested under monotonic loading conditions. The second one has instead been subjected to stepwise increasing deformation cycles. The cyclic loading history has been inspired to the ATC-24 [1] testing protocol, but the deformation amplitudes have been defined in such a way to reproduce some characteristic values of deformation demand parameters found through a numerical analysis simulating the effects of 26 natural acceleration records.

INTRODUCTION

Commonly, in cold-formed lightweight steel houses the lateral load resisting systems are Sheathed Cold-Formed Steel Stud Shear Walls (SCFSSSWs), which in the following will be briefly indicated as Sheathed Stud Walls (SSWs). These shear walls are generally obtained by the assembling of single internal and coupled back-to-back external profiles (studs) having a lipped channel cross-section. The studs are interconnected at each end by members (tracks) having unlipped channel cross-sections, in such a way to realize a cold-formed steel frame called 'stud wall'. This frame is usually sheathed with wood-based and/or gypsum-based panels but, in some cases, also steel sheets or composite sandwich panels are used.

Many experimental programs have been carried out in the past on steel stud shear walls with different assemblies [2,3,4,5,6,7,8,9,10,11,12,13,14,15,16,17,18,19]. These investigations have included various topics. The basic behaviour of different sheathing types (including walls sheathed with plywood, oriented strand board, gypsum wallboard, gypsum sheathing board, steel sheet sheathing and fiberboard) with different thicknesses has been examined by Tarpy [4], Tarpy and Girard [5], Serrette *et al.* [8,9,10,11],

---

[1] Full professor, Department of Construction and Mathematical Methods in Architecture, University of Naples "Federico II", Naples, Italy.
[2] Assistant professor, Department of Structural Analysis and Design. University of Naples "Federico II", Naples, Italy.
[3] Eng., Ph.D., Department of Structural Analysis and Design. University of Naples "Federico II", Naples, Italy.

Salenikovich *et al*. [16] and Dubina and Fulop [18]. Studies on the influence of sheathing orientation and the contribution of horizontal steel straps and blocking installed at mid-height of the walls have been presented by Serrette and Ogunfunmi [8] and Serrette *et al*. [11]. Tarpy and Girard [5], Tissell [6] and Serrette *et al*. [13] discuss the effect of framing stud size, thickness and spacing. The contribution of steel flat strap tension X-bracing has been analysed by Serrette and Ogunfunmi [8], Serrette *et al*. [13] and Gad *et al*. [14]. Extensive studies on the effect of fasteners' type, size and spacing have been presented by Tarpy and Hauenstein [3], Tarpy [4], Tarpy and Girard [5], Tissell [6], Serrette *et al*. [9,10,11,12], Gad *et al*. [14] and COLA-UCI [17]. McCreless and Tarpy [2], Tarpy and Girard [5] and Serrette *et al*. [9,12] evaluate the effect of the wall aspect ratio variation, while in NAHB Research Center [13], Salenikovich *et al*. [16] and Dubina and Fulop [18], the influence of the opening size is presented. The effect of cyclic loading on the lateral behaviour has been investigated by Serrette *et al*. [9,10,12], Gad *et al*. [14,15], Salenikovich *et al*. [16], COLA-UCI [17], Dubina and Fulop [18] and Branston *et al*. [19]. A deep review of existing experimental research on cold-formed steel stud shear walls is given in Zhao [20] and Fiorino [21].

The examination of these existing experimental studies demonstrates the existence of a relatively large database of results. However, several aspects still need investigation. For example, looking at the relatively small ratio between the number of studies dealing with the cyclic behaviour and those dealing with the monotonic one, it can be argued that some lacking of knowledge about the seismic response still exists. Moreover, following subjects deserve further investigation: a) analysis of the efficiency of the horizontal load transfer from the floor to the vertical stud shear walls; b) effect of the level of gravity load on the lateral response of walls; c) study of constructional details. Besides, a relatively small number of studies has been dedicated to evaluate seismic deformation demand.

As an attempt to face some of the above issues, a specific research program, aiming at characterizing the capacity and demand of this structural system, has been planned. The research program has been articulated in two main phases. The first phase is the experimental one. It consisted of full-scale static (both monotonic and cyclic) tests on SSW sub-assemblages. The second phase consists in a numerical study focused on the evaluation of seismic demand to SSW systems.

This paper mainly presents the results of the first experimental phase.

THE EXPERIMENTAL INVESTIGATION

Testing program

Specimens

Physical tests have been carried out on two nominally identical wall sub-assemblages [22]. One sub-assemblage has been tested, up to collapse, under a monotonically increasing lateral load. The second one has been instead subjected to a purposely developed cyclic loading history. The generic sub-assemblage is shown in Figure 1. It can be considered as a good prototype of typical lateral load resisting systems of house structures built with cold-formed steel framing and sheathed with panels. In particular, Figure 1a illustrates the specimen without panels. Figure 1b shows, instead, the specimen sheathed with floor and wall panels.

Specimens were designed according to the Prescriptive Method For Residential Cold-Formed Steel Framing [23]. The generic wall framing, which was 2400mm long and 2500mm height, consisted of single top and bottom tracks, single intermediate studs and double back-to-back end studs, spaced 600mm on centre. The floor framing consisted of joists spaced 600mm on centre, with single span of 2000mm. The foundation was simulated by two 280x380mm (depth x width) rectangular concrete beams. The walls were connected to the foundation by intermediate shear anchors and purposely-designed steel hold-down connectors placed in correspondence of the end studs. All frame members were cold-formed, fabricated

from FeE350G (S350GD+Z/ZF) [24] hot dipped galvanized (zinc coated) grade steel (nominal yield strength f_y=350MPa and nominal tensile strength f_t=420MPa). Wall and floor external sheathings were made by type 3 oriented strand board (OSB/3) [25], whereas internal sheathings of the wall were made by gypsum wallboard (GWB) [26].
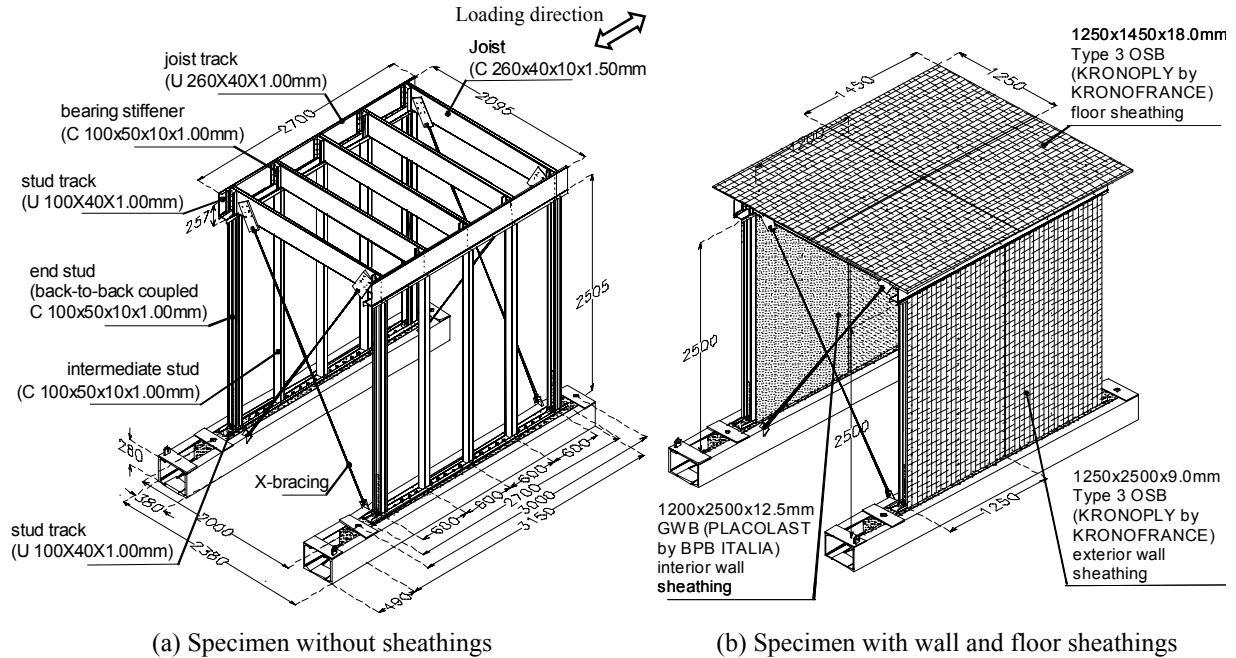
(a) Specimen without sheathings   (b) Specimen with wall and floor sheathings
Figure 1. Global 3D view of the generic sub-assemblage.

All the stud shear wall sub-assemblage components (members, panels and connections) were designed according to capacity design principles, in such a way to promote the development of the full shear strength of sheathing-to-wall framing connections. For this reason, shear anchors and hold-down connectors were designed to prevent either shear failure at the base of the walls or failure due to overturning. Besides, double lipped C-sections at the ends of the walls were adopted, in order to avoid failure due to buckling in end studs. Main details of the specimen components are reported in Table 1 [21].

Test setup
Two types of load were applied: gravity and racking loads. A gravity load of 45kN was applied on the floor of the prototype. This load was computed starting from the dead (including roof, floor and walls), snow and live loads applied to the plan area of a typical one-family one-story house, in such a way to reproduce typical values of gravity-induced axial forces in the studs. Racking loads were applied to the floor panels by means of two programmable servo-hydraulic actuators (MTS System Corporation) with the range of displacement of 500mm. The actuators' forces were transformed into a distributed load applied to the floor panels by means of a purposely-designed load transfer steel system, which is shown in Figure 2. A sliding-hinge was placed between the actuators and the structure in order to avoid the introduction of additional vertical load components in the tested system. This testing apparatus allowed the capacity of the horizontal floor panels to transmit loads to the vertical wall panels to be checked, up to failure of the vertical stud-to-panel connections.

Tests were carried out at the Department of Structures, Geotechnique, Applied Geology of the University of Basilicata.

Table 1. Full-scale specimen materials and construction data.

Cold formed steel members		
Steel grade	FeE350G (S350GD+Z/ZF) hot dipped galvanized (zinc coated) steel (Nominal yield strength f_y=350MPa; nominal tensile strength f_t=420MPa)	
Wall members	Studs	C (lipped channel section) 100x50x10x1.00mm (web depth x flange size x lip size x thickness) (2400mm long) [1]
	Tracks	U (unlipped channel section) 100x40x1.00mm (web depth x flange size x thickness) (2700mm long) [1]
Floor members	Joist	C 260x40x10x1.50mm (2200mm long) [1]
	tracks	U 260x40x1.00mm (2700mm long) [1]
	Bearing stiffeners	C 100x50x10x1.00mm (260mm long) [1]
Sheathings		
Wall sheathings	Interior	1200x2500x12.5mm (width x height x thickness) GWB (PLACOLAST) vertically oriented [2]
	Exterior	1250x2500x9.0mm Type 3 OSB (KRONOPLY 3) vertically oriented [3]
Floor sheathing		1250x2500x18.0mm Type 3 OSB (KRONOPLY 3) vertically oriented [3]
Concrete beams foundation		
Concrete type	C20/25 (characteristic strength on a cube 150x150x150mm $f_{ck,cube}$=25MPa)	
Dimensions	380x280mm rectangular section (3590mm long)	
Frame-to-foundation connections		
Hold-down connector	Purposely-designed welded steel hold-down	
Hold-down anchors	HIT-RE 500 with HIS-N(8.8) M20 adhesive-bonded anchors [4]	
Shear anchors	HST M8 mechanical anchors spaced at 100mm [4]	
Steel-to-steel connections		
CFS members	4.2x13mm (diameter x lenght) modified truss head self drilling screws [5]	
CFS members-to-hold down connector	6mm diameter bolts	
Steel-to-Sheathing connections		
Walls	Interior	3.5x25mm bugle head self drilling screws spaced at 150mm at the perimeter and at 300mm in the field [5]
	Exterior	4.2x25mm flat head self drilling screws spaced at 150mm at the perimeter and at 300mm in the field [5]
Floor		4.2x32mm flat head self drilling screws spaced at 150mm for sheathing-to-track connections and at 250mm for sheathing-to-joist connections [5]

[1] manufactured by the Company GUERRASIO, Italy
[2] manufactured by the Company BPB ITALIA
[3] manufactured by the Company KRONO FRANCE
[4] manufactured by the Company HILTI ITALIA
[5] manufactured by the Company TECFI s.r.l., Italy

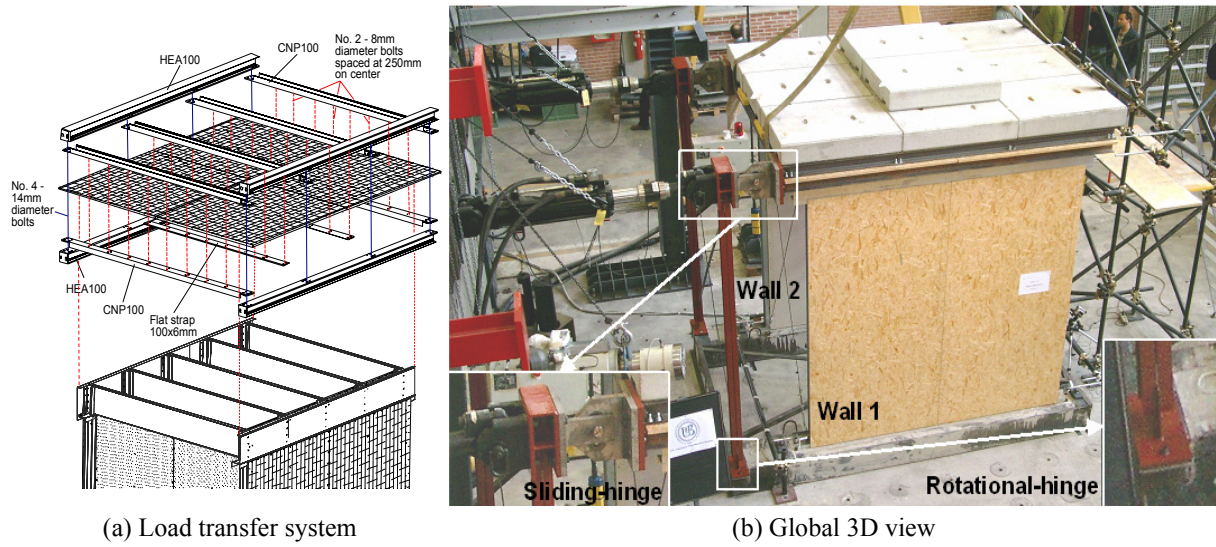(a) Load transfer system   (b) Global 3D view

Figure 2. Test setup.

Instrumentation

Fourteen potentiometers were used for measuring displacements of the specimens during tests, as shown in Figure 3. In particular, five potentiometers were installed for each wall (Fig. 3a): the potentiometer w1 was used for measuring the horizontal displacements at the top of the wall (lateral in-plane displacement); potentiometers w2 and w3 measured the horizontal displacements at the bottom of the wall (lateral in-plane sliding); potentiometers w4 and w5 measured the vertical displacements at the bottom of the wall (uplift and compression). One potentiometer (f1) was installed for each foundation beam (Fig. 3a) in order to measure the horizontal sliding of the foundation. Finally, two potentiometers (d1 and d2) were installed on the floor (Fig. 3b), in order to measure its lateral displacements.

(a) Walls   (b) Floor

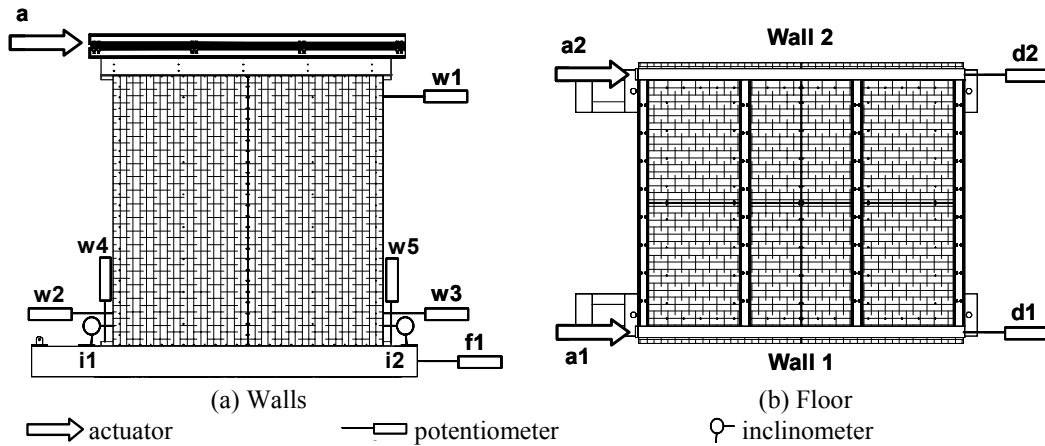⇨ actuator   ▭ potentiometer   φ inclinometer

Figure 3. Instrument arrangement.

Horizontal displacements of the floor (d1 and d2) and walls (w1, w2 and w3) were measured using potentiometers with a range of 250mm and an accuracy of 0.02mm. For measuring horizontal displacements of foundations (f1 and f2) potentiometers with a range of 100mm and an accuracy of 0.01mm were used. Finally, vertical displacements of walls (w4 and w5) were measured using potentiometers with a range of 20mm and an accuracy of 0.01mm. The load was measured through the actuators' load cells. Data, were acquired at 20Hz.

Loading conditions
Two loading protocols were applied in the testing of the specimens: monotonic and cyclic.

In the monotonic loading regime, the specimen was subjected to progressive horizontal deflection. In particular, the loading procedure for the monotonic test was articulated in two phases. In the first phase, in order to evaluate the permanent set at 2, 4, 6 and 10mm, the specimen was unloaded at these displacements. In the second phase, the specimen was monotonically loaded up to a displacement of 150mm. This testing protocol involved displacements at a rate of 0.10mm/s, for displacements less than 10mm, and of 0.20mm/s, for displacements exceeding 10mm.

As it is well known, an experiment can provide information on capacities. But, because of the strong interrelation between capacity and demand, due consideration must be given to seismic demand issues when designing a seismic performance evaluation test [27]. Therefore, a specific study on seismic deformation demand to the system under investigation has been carried out, with the aim to develop a testing-protocol taking into account the effect of non-linearity (also for small deformations) and pinching of hysteresis loops on seismic demand. The numerical analysis has been carried out using the numerical model presented in [28]. This model has been calibrated using data coming from both the monotonic test previously performed and the existing available data on cyclic tests. The choice of the loading history has been based on the following cumulative damage parameters: the number of inelastic excursions (N_p), the sum of normalized plastic deformation ranges ($\Sigma \Delta d_{pi}/d_y$), the ratio between the mean value (($\Delta d_p)_{av}$) and the maximum value (($\Delta d_p)_{max}$) of the plastic deformation range (($\Delta d_p)_{av}/(\Delta d_p)_{max}$). 26 natural acceleration records have been used. They were recorded during the Lazio-Abruzzo (1984) and Umbro-Marchigiano (1997) earthquakes. Records have been chosen in such a way to cover all the soil types defined by Eurodode 8 [29]. Each accelerogram has been scaled in such way that the elastic spectral acceleration (S_{ae}), be equal to the spectral acceleration inducing the ultimate lateral displacement (S_{aeu}) as measured in the monotonic test. Results of the statistic characterization of the cumulative damage parameters are synthesized in Figures 4 a through c. In particular, the number of inelastic excursions (N_p) (Fig. 4a), the sum of normalized plastic deformation ranges ($\Sigma \Delta d_{pi}/d_y$) (Fig. 4b), and the ratio between the mean value and the maximum value of the plastic deformation range (($\Delta d_p)_{av}/((\Delta d_p)_{max}$) (Fig. 4c) are reported for each accelerogram. Also the mean and the standard deviation values have been calculated for all earthquake records. As it is shown in Figures 4a, b and c, N_p ranges from 10 to 53 with a mean and standard deviation values of 25 and 12, respectively; the range of $\Sigma \Delta d_{pi}/d_y$ is from 5.8 to 9.5 with a mean value of 7.2 and a standard deviation of 0.9; finally, (($\Delta d_p)_{av}/((\Delta d_p)_{max}$ ranges from 0.06 to 0.41 and its mean and standard deviation values are 0.23 and 0.10, respectively.

The developed cyclic loading test protocol consists of a series of stepwise increasing deformation cycles, following a procedure similar to the one described in [1] for a multiple step test. The displacement amplitudes were fixed in such a way to reproduce, in the physical test, as close as possible, the mean values of the cumulative damage parameters (N_p, $\Sigma \Delta d_{pi}/d_y$, (($\Delta d_p)_{av}/(\Delta d_p)_{max}$) obtained by the numerical study. The designed loading history is characterised by N_p=25, and $\Sigma \Delta d_{p,i}/d_y$=6.2. and (($\Delta d_p)_{av}/(\Delta d_p)_{max}$)=0.28, if these value are computed on the basis of the numerical simulation of the physical test.

The designed loading history is characterised by three cycles of fully reversing, displacement-controlled, load at each wall displacement increment representing 25%, 50% and 75% of the conventional yield limit state (YLS) displacement (d_y=6.0mm). Then, the wall displacement was increased for three loading cycles to 100% of the YLS displacement. Next, the lateral displacement was increased at 150%, 200%, 300%, 400% and 600% of the YLS displacement, repeating three cycles for each amplitude. At this point the loading history based on the statistic characterization of deformation demand was completed. However, to capture the behaviour of the specimen under larger displacement amplitudes, the displacement was further

increased at 700%, 800%, 900%, 1000%, 1100%, 1200%, and 1300% of the YLS displacement always repeating three cycles for each amplitude. The adopted test protocol is depicted in Figure 4d. It involved displacements at a rate of 2.00mm/s.
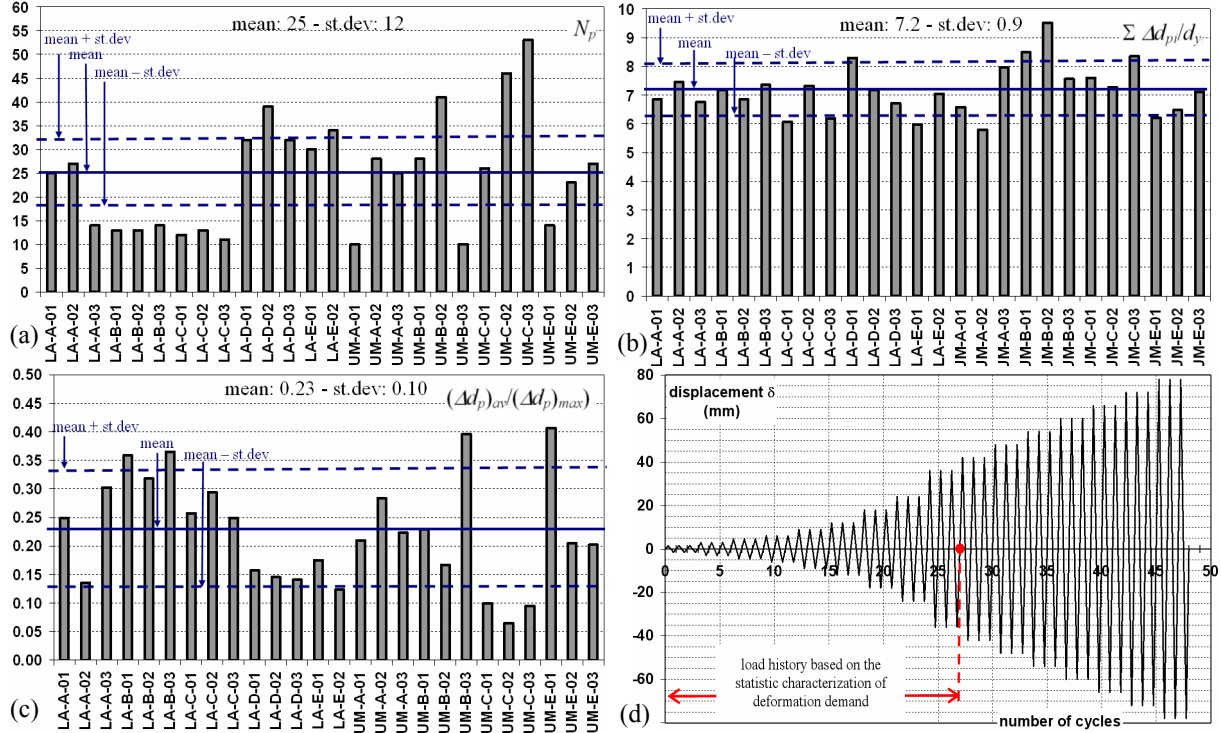

Figure 4. Establishing the cyclic loading history.

Test Results

The monotonic test

The global behaviour of the sub-assemblage under monotonic racking loads may be synthesized by means of the relationship between the measured unit shear resistance (v) and the mean displacement (*d*) of the specimen. In particular, the value of v and *d* are defined as:

$$v = \frac{V_1 + V_2}{L_t} \text{ and } d = \frac{d_1 + d_2}{2} \tag{1}$$

where: V_1 and V_2 are the forces measured by the actuators a1 and a2, respectively; d_1 and d_2 are the displacements measured by the actuators a1 and a2, respectively; L_t=4800mm is the total length of the walls.

The v-*d* response curve is showed in Figure 5a. In the same Figure, four important loading steps are highlighted:

- Step 1: lateral displacement equal to 10mm. At this step, in the OSB sheathing-to-frame connections tilting of the screws about the plane of the stud flange started, while for the GWB sheathing-to-frame connections bearing of the GWB panels begun. At this displacement level, global deformation of walls as well as local deformations of the sheathing-to-frame connections were not evident.
- Step 2: maximum shear resistance (lateral displacement equal to 36mm). At this loading step global deformation of walls was clearly observable, as shown in Figure 6a. Tilting of screws in the OSB connections, as well as bearing in the GWB panels were evident, as shown in Figures 6 b and c, respectively.

- Step 3: lateral displacement equal to 80mm. At this displacement level, in both the OSB and GWB-to-frame connections screw heads initiated to pull through the sheathings. At this point, owing to the rotation of the sheathings, the upper sides of the GWB panels knocked against the joist. This phenomenon could probably explains the residual shear resistance exhibited for displacements varying from 70 to 110mm.
- Step 4: lateral displacement equal to 130mm. At this step, the screw heads completely pulled through the sheathings, as shown in Figures 7 b and c. As a consequence, the sheathings were completely unzipped along the panel edges.
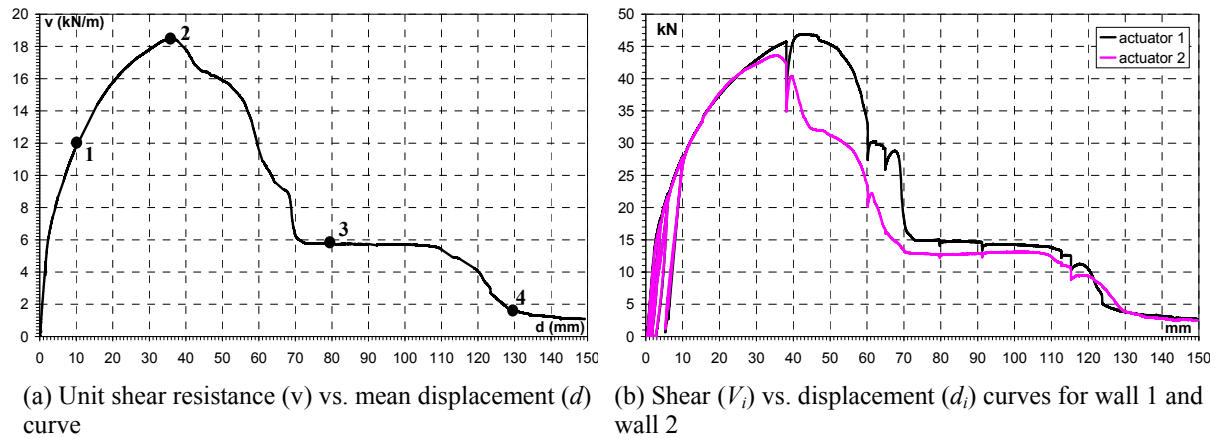

(a) Unit shear resistance (v) vs. mean displacement (d) curve
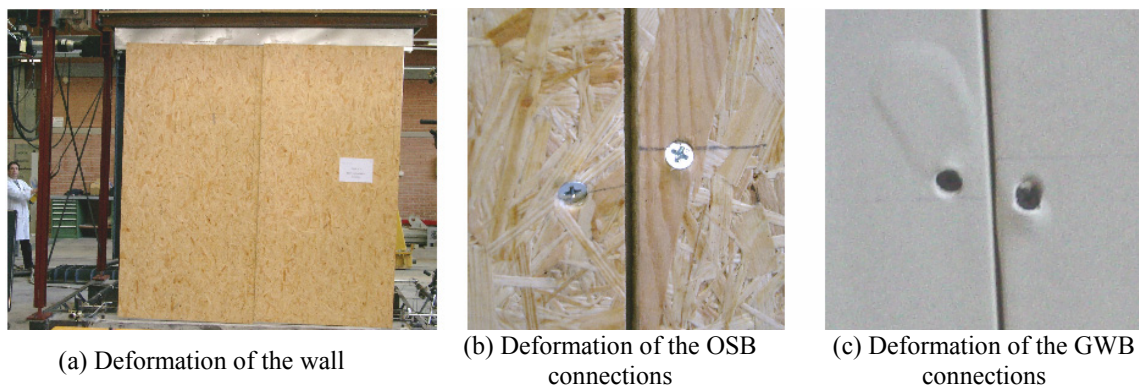

(b) Shear (V_i) vs. displacement (d_i) curves for wall 1 and wall 2

Figure 5. Monotonic shear response.

(a) Deformation of the wall

(b) Deformation of the OSB connections

(c) Deformation of the GWB connections

Figure 6. Specimen condition at Step 2 (maximum shear resistance - d=36mm) of the monotonic test.

(a) Deformation of the wall

(b) Deformation of the OSB connections
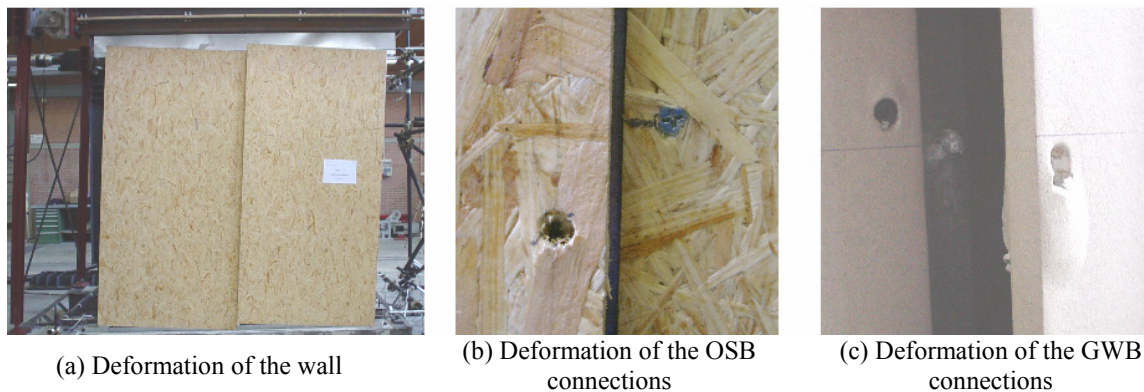

(c) Deformation of the GWB connections

Figure 7. Specimen condition at Step 4 (d=130mm) of the monotonic test.

For all displacement levels, the evolution of the deformation of the specimen was consistent with the sheathing-to-wall framing connections failure. In fact, wall framing deformed into a parallelogram and the sheathings had rigid body rotation, as shown in Figures 6a and 7a. No buckling phenomena were observed for the studs as well as deformations of the OSB sheathing-to-floor framing connections. On the contrary, for floor tracks, a web local buckling phenomenon occurred for lateral displacements larger than about 30mm. Moreover, both the shear and the tension foundation anchors did not suffer any type of failure.

The load transfer system between the floor and the walls was very effective: in fact, the floor-to-walls sliding (given by the difference of measures taken by potentiometers d_i and $w_{1,i}$) was relatively small. Figure 5b shows the comparison of the force (V_i) vs. displacement (d_i) response curves obtained for each of the two tested walls. The two walls had the same behaviour for displacements less than about 30mm (displacement for which the applied load approached the maximum shear resistance), while they exhibited different response for larger displacements. The maximum shear resistances of the two walls were very similar (47 and 44kN for wall 1 and 2, respectively) as well as displacements corresponding to peak strength.

The cyclic test
The global cyclic response in terms of unit shear resistance (v) vs. mean displacement (*d*) curve is shown in Figure 8a. In this Figure, v_{MAX+1} represents the maximum (positive) unit shear measured during the whole loading history; v_{MAX+3} represents the positive unit shear measured at the third cycle of displacement corresponding to v_{MAX+1}; v_{MAX-1} and v_{MAX-3} are the analogous quantities measured in the opposite direction of loading (negative values). Positive values v are relevant to the direction of the first loading of the structures. In particular, the experimental maximum loads were obtained for a lateral displacement of +36mm. The relevant forces resulted v_{MAX+1}=+16.4kN/m and v_{MAX+3}=+10.2kN/m for the first and third cycle, respectively. For the negative loads, the minimum values were found for a lateral displacement of -24mm. Their values were v_{MAX-1}=-14.8kN/m and v_{MAX-3}=-12.5kN/m for the first and third cycle, respectively. The cumulative damage parameters, computed on the basis of the physical test results, are N_p=32, and $\Sigma\Delta d_{p,i}/d_y$=7.5 and $(\Delta d_p)_{av}/(\Delta d_p)_{max}$=0.14.
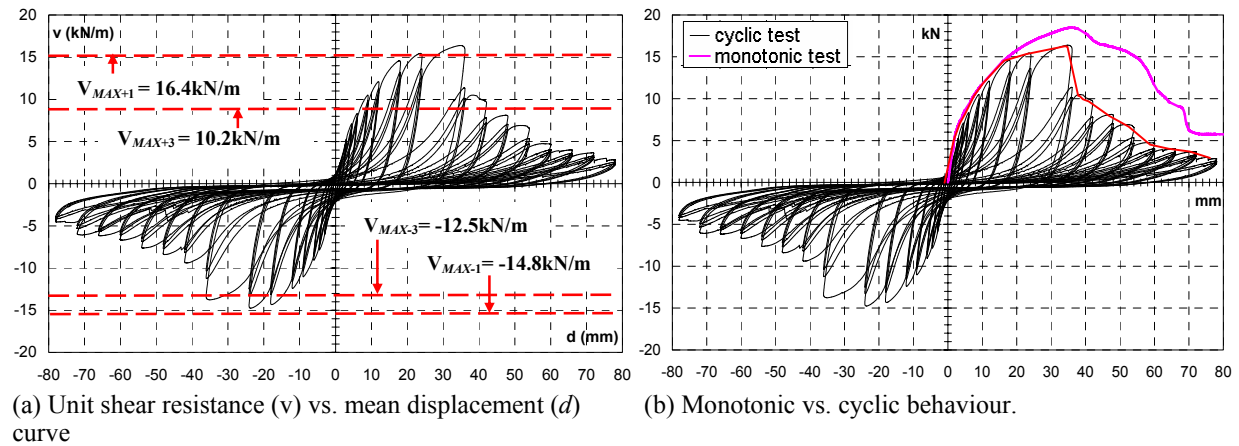

(a) Unit shear resistance (v) vs. mean displacement (*d*) curve

(b) Monotonic vs. cyclic behaviour.

Figure 8. Cyclic shear response.

From the comparison between the experimental loads obtained at the first (v_{MAX+1} and v_{MAX-1}) and third (v_{MAX+3} and v_{MAX-3}) cycle of loading, a reduction of 38% and 16% for positive (v_{MAX+1} vs. v_{MAX+3}) and negative (v_{MAX-1} vs. v_{MAX-3}) shear strengths is noted. These results highlight the strong shear strength degradation occurring after attainment of the peak load was achieved.

During the test two different behaviours were identified:

- For lateral displacements less than the ones corresponding to the maximum shear resistance, the behaviour of OSB sheathing-to-frame connections resulted from a combination of the tilting of the screws about the plane of the stud flange and the screw heads pulling through the OSB sheathings. The response of the GWB sheathing-to-frame connections was characterized by a combination of the bearing of the GWB panels and the screws' heads pulling through the GWB panels. For these displacement levels the skeleton-to-panel deformation was congruent. In fact, the wall framing deformed into a parallelogram and the sheathings had rigid body rotation.
- For lateral displacements larger than the one corresponding to the maximum shear resistance, the heads of the end screws completely pulled through the sheathings in the upper half of the walls or, in some cases, the screws caused the rupture of the sheathing edges. As a result, both the OSB and GWB sheathings became unzipped along the panel edges in the upper half of the specimen (see Fig. 9a). Moreover, for displacement levels larger than 42mm also distortional buckling phenomena in the end studs of the wall 1 were observed, as shown in Figure 9b. For these displacement levels the deformation of the wall framing still had the shape of a parallelogram, while due to the rupture of sheathing-to-frame connections, the rotation of the sheathings was limited, as shown in Figure 9c. As in the case of monotonic test, no appreciable deformation of the OSB sheathing-to-floor framing connections was observed and both the shear and the tension anchors did not suffer any type of failure.

(a) Unzipping of sheathings   (b) Distortional buckling of end studs   (c) Wall deformation
Figure 9. Specimen condition at failure in the case of the cyclic test.

By comparing the lateral response of the two walls, observations similar to those deduced from the monotonic test are possible. In fact, the walls had a similar behaviour until displacements corresponding to the maximum shear resistance (36mm) were approached, while they exhibited different responses for larger displacements.

Monotonic vs. cyclic responses
The comparison between the monotonic and cyclic behaviour is shown in Figure 8b. In this Figure both the cyclic and monotonic response are synthesized by means of the unit shear resistance (v) vs. mean displacement (*d*) curves. In particular, v_{MAX+1} and v_{MAX-1} were 11% and 20% smaller than the peak strength measured in the monotonic test, respectively. The strength degradation after the achievement of the peak strength was much more evident in the cyclic loading test, with respect to the monotonic case. This is well evidenced by the comparison between the unstable part of response in the monotonic and cyclic regimes of loading. For example, v_{MAX+3} and v_{MAX-3} were 45% and 32% smaller than the monotonic peak strength, respectively.

CONCLUSIONS

An experimental investigation on sheathed cold-formed steel stud shear walls has been presented and discussed throughout the current paper. The obtained results allow the following conclusions to be drawn:

- All the components of this structural system can be designed according to capacity design principles, imposing collapse in the vertical shear walls' connections (most ductile collapse mechanism), without significant increase of the cost. In fact, the evolution of the deformation of both tested specimens was consistent with the sheathing-to-wall framing connections failure.
- In the monotonic test the collapse mechanism was invariant during the increasing lateral displacement, whilst in the cyclic test some modifications occurred after that the peak lateral load was achieved. In fact, in the cyclic test, the wall-to-framing connections in the upper part of the wall failed before than the ones in the lower part. Consequently the panels became unzipped in the upper half of the wall inducing a distortional buckling phenomenon in the end studs. As a consequence, strength degradation in the cyclic test, after the achievement of the peak load, was stronger than the one observed during the monotonic test.
- The lateral-load response for displacements lesser than the ones corresponding to the peak strength was very similar for all tested walls, whilst significant differences were observed for larger values of the displacement. This indicates a relatively more unreliable response in the unstable branch of the behaviour.
- The horizontal diaphragm (made of a simple wood-based sheathing fastened with bugle head self-drilling screws to horizontal cold-formed girders) can adequately transfer the horizontal loads to the of vertical shear walls, without any appreciable damage. In fact, no appreciable deformation of the OSB sheathing-to-floor framing connections was observed in both monotonic and cyclic tests.

ACKNOWLEDGEMENTS

REFERENCES

1. *Guidelines for cyclic seismic testing of components of steel structures (ATC-24)*. ATC, Redwood City, CA, 1992.
2. McCreless S, Tarpy TS. Experimental investigation of steel stud shear wall diaphragms. In Proceedings of the *4th International Specialty Conference on Cold-formed Steel Structures*. St. Louis, MO, 1978.
3. Tarpy TS, Hauenstein SF. *Effect of construction details on shear resistance of steel-stud wall panels*. Research project sponsored by AISI. Project No.1201-412, 1978.
4. Tarpy TS. Shear resistance of steel-stud wall panels. In Proceedings of the *5th International Specialty Conference on Cold-formed Steel Structures*. St. Louis, MO, 1980.
5. Tarpy TS, Girard JD. Shear resistance of steel-stud wall panels. In Proceedings of the *6th International Specialty Conference on Cold-formed Steel Structures*. St. Louis, MO, 1982.
6. Tissell JR. *Wood structural panel shear walls*. Report No.154, APA, Tacoma, WA, 1993.
7. Serrette R. *Light gauge steel shear wall test*. Light Gauge Steel Research Group, Department of Civil Engineering, Santa Clara University. Santa Clara, CA, 1994.
8. Serrette RL, Ogunfunmi K. Shear resistance of gypsum-sheathed light-gauge steel stud walls. *Journal of structural engineering*, ASCE 1996, Vol.122, No.4: 386-389.
9. Serrette R, Nguyen H, Hall G. *Shear wall values for light weight steel framing*. Report No.LGSRG-3-96, Department of Civil Engineering, Santa Clara University. Santa Clara, CA, 1996.

10. Serrette R, Hall G, Nguyen H. Dynamic performance of light gauge steel framed shear walls. In Proceedings of the *13th International Specialty Conference on Cold-formed Steel Structures*. St. Louis, MO, 1996.

11. Serrette RL, Encalada J, Juadines M, Nguyen H. Static racking behavior of plywood, OSB, gypsum, and fiberboard walls with metal framing. *Journal of Structural Engineering*, ASCE 1997, Vol.123, No.8: 1079-1086.

12. Serrette R, Encalada J, Matchen B, Nguyen H, Williams A. *Additional shear wall values for light weight steel framing*. Report No.LGSRG-1-97, Department of Civil Engineering, Santa Clara University. Santa Clara, CA 1997.

13. *Monotonic Tests of cold-formed steel shear walls with openings*. NAHB, Upper Marlboro, MD, 1997.

14. Gad EF, Duffield CF, Hutchinson GL, Mansell DS, Stark G. Lateral performance of cold-formed steel-framed domestic structures. *Engineering Structures*, Elsevier 1999, Vol.21, No.1: 83-95.

15. Gad EF, Chandler AM, Duffield CF, Stark G. Lateral behaviour of plasterboard-clad residential steel frames. *Journal of Structural Engineering*, ASCE 1999, Vol.125, No.1: 32-39.

16. Salenikovich AJ, Dolan JD, Easterling WS. Racking performance of long steel-frame shear walls. In Proceedings of the *15th International Specialty Conference on Cold-formed Steel Structures*. St. Louis, MO, 2000.

17. *Report of a testing program of light-framed walls with wood-sheathed shear panels*. Final report to the City of Los Angeles Department of Building and Safety, Structural Engineers Association of Southern California. Irvine, CA, 2001.

18. Dubina D, Fulop LA. Seismic performance of wall-stud shear walls. In Proceedings of the *16th International Specialty Conference on Cold-formed Steel Structures*. St. Louis, MO, 2002.

19. Brantson A, Boudreault F, Rogers CA. *Testing on steel frame / wood panels shear walls*. Progress Report, Departement of Civil Engineering and Applied Mechanics, McGill University. Montreal, 2003.

20. Zhao Y. *Cyclic performance of Cold-Formed Steel Stud Shear Walls*. MSc. Thesis, Department of Civil Engineering and Applied Mechanics, McGill University, Montreal, 2002.

21. Fiorino L. *Seismic Behavior of Sheathed Cold-Formed Steel Stud Shear Walls: An Experimental Investigation*. Ph.D. Dissertation, Department of Structural Analysis and Design, University of Naples "Federico II", 2003.

22. Della Corte G, Fiorino L, Landolfo R, Di Lorenzo G. Seismic performance of steel stud shear walls: planning of a testing program. In proceedings of the *4th International Conference on Behavior of Steel Structures in Seismic Areas (STESSA 2003)*. Napoli.

23. *Prescriptive Method For Residential Cold-Formed Steel Framing (Year 2000 Edition)*. NASFA, Lexington, KY.

24. EN 10142 *Continuously hot-dip zinc coated low carbon steel sheet and strip for cold forming. Technical delivery conditions*. CEN, Bruxelles, 2002.

25. EN 300 *Oriented Strand Boards (OSB) - Definitions, Classification and Specifications*. CEN, Bruxelles, 1997.

26. ISO *Gypsum plasterboard – Specification*. ISO, Geneva, 1980.

27. Krawinkler H. Cycling loading histories for seismic experimentation on structural components. *Earthquake Spectra 1996*, Vol. 12, No. 1: 1-12.

28. Della Corte G, De Matteis G, Landolfo R. Influence of connection modeling on seismic response of moment resisting steel frames. In F.M. Mazzolani (ed.), *Moment resistant connections of steel building frames in seismic areas*. E & FN SPOON, 2000.

29. prEN 1998-1: *Eurocode 8: Design of structures for earthquake resistance – Part 1: General rules – Seismic actions and rules for buildings*. CEN, Bruxelles. (final draft December 2003).